Optics Letters

Adaptive intensity transformation-based phase retrieval with high accuracy and fast convergence

Meng Xiang,[1] Peijian Zhou,[1] Bolin Ye,[2] Songnian Fu,[1,*] Ou Xu,[1] Jianping Li,[1] Di Peng,[1] Yuncai Wang,[1] and Yuwen Qin[1]

[1]Advanced Institute of Photonics Technology, School of Information Engineering, and Guangdong Provincial Key Laboratory of Information Photonics Technology, Guangdong University of Technology, Guangzhou 510006, China
[2]Shenzhen Techwinsemi Optoelectronic Co., Ltd., Shenzhen 518000, China
*Corresponding author: songnian@gdut.edu.cn

Received 3 June 2021; accepted 8 June 2021; posted 10 June 2021 (Doc. ID 433349); published 28 June 2021

Phase-retrieval (PR) receivers can reconstruct complex-valued signals from two de-correlated intensity measurements, without the assistance of any optical carriers. However, both the calculation complexity with hundreds of iterations and the limited PR accuracy prevent it from being applied to high-speed photonic interconnections. Here we propose and demonstrate a PR receiver based on adaptive intensity transformation, with the capability of both fast convergence and high accuracy. Then we numerically reconstruct 56 GBaud QPSK signals after the 80 km standard single-mode fiber transmission by using our proposed PR receiver with only 50 iterations. In comparison with the recently reported PR receiver with the phase reset, our proposed PR receiver can reduce the required optical signal-to-noise ratio by 1.95 and 1.89 dB, in terms of 20% soft-decision and 7% hard-decision forward-error correction, respectively.

https://doi.org/10.1364/OL.433349

The explosive growth of multimedia applications stimulates the anticipation for high-speed large-capacity fiber optical communication systems. For the short-reach photonic interconnections, intensity modulation direct detection (IM-DD) transmission has been widely employed due to its simple configuration, low cost, and small power consumption. However, because of the square-law detection during the optical-to-electrical conversion, the chromatic dispersion (CD) induced power fading can significantly deteriorate the signal quality, leading to a reach constraint of the high-speed IM-DD transmission system by a several-kilometer standard single-mode fiber (SSMF). Aiming to extend the achievable SSMF reach, it is highly desired to digitally compensate for the CD when the optical field information can be completely reconstructed at the receiver side (Rx) [1].

To correctly recover the optical signal field from its intensity measurement, one approach named the self-coherent Stokes vector detection first gained extensive research interest, where a carrier is inserted at the transmitter side (Tx) and propagated over the SSMF with the modulated signals [2]. However, the Stokes vector detection needs at least three single-ended photodiodes (PDs) and an optical hybrid. Another approach for the recovery of the optical signal field is to insert a strong optical carrier together with the single-sideband modulation signal. After the direct detection based on a single-ended PD, the phase of the optical signal can be retrieved from the intensity measurement according to the well-known Kramers–Kronig (KK) relationship [3]. However, in order to maintain the recovery performance of the optical field, a strong optical carrier is fundamentally essential, thus leading to a higher carrier-to-signal power ratio (CSPR) and an additional penalty of receiver sensitivity. Research efforts have been carried out to reduce the CSPR [4,5], but more than 3 dB CSPR is still required for the correct recovery of the optical field. Recently, a scheme to circumvent such a carrier requirement, which is called a carrier-less phase retrieval (PR) receiver, has been proposed and investigated [6–10]. Please note that the carrier-less PR receiver may use 1 and 2 PDs for a one-dimensional OOK signal [6] and two-dimensional QAM signal [7,10], respectively. Generally speaking, the complete optical signal field can be recovered via multiple intensity-only measurements under different projections. After each projection, by adding CD, the signal intensity is de-correlated, and the signal phase can be retrieved, when the PR algorithm keeps iteratively running until the intensities of the reconstructed signal at all projection planes agree with the measurement results [6,11]. Previous studies have shown that one projection is enough for the PR of QAM signals, in order to reduce the implementation complexity. However, the performance of the PR receiver, in terms of both the convergence speed and the PR accuracy, needs further improvement [7].

In this submission, we propose an adaptive intensity transformation (AIT)-based PR receiver (PR_AIT) with a fast convergence and a high PR accuracy, under the condition of two CD-assisted de-correlated intensity measurements. Compared with the newly reported PR receiver with the phase reset (PR_PR) [10], both the convergence speed and the steady bit-error-rate (BER) performance are significantly improved.

Figure 1 shows the schematic illustration of the PR receiver with two intensity measurements, which composes an optical splitter, a dispersive element, and two single-ended PDs. The optical signal detected by the first PD and the second PD can be separately written as

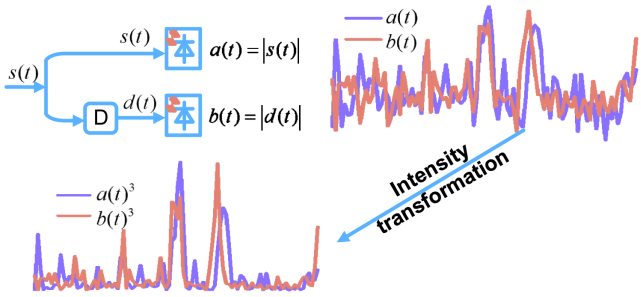

Fig. 1. Illustration of the carrier-less PR receiver and intensity transformation process.

$$s(t) = \sum_k x_k \cdot g(t - kT) + n(t), \tag{1}$$

$$d(t) = \sum_k x_k \cdot \hat{g}(t - kT) + \hat{n}(t), \hat{g}(t) = g(t) * h_D(t), \tag{2}$$

where x_k represents the complex-valued data symbols, T is the symbol duration, and $g(t)$ is the fundamental pulse waveform, including the CD effect due to the SSMF transmission; $n(t)$ and $\hat{n}(t)$ denote the additive noise accumulated from the SSMF link, respectively. $h_D(t)$ is the complex transfer function induced by the use of the dispersive element, and the Fourier transform of $h_D(t)$ is

$$H_D(f) = fft(h_D(t)) = \exp(-j\pi D_D \lambda^2 f^2/c), \tag{3}$$

where λ is the operation wavelength of the semiconductor laser, c is the light propagation speed in vacuum, and D_D is the additional CD value from the dispersive element. Generally, the goal of the PR receiver is to reconstruct $s(t)$ from two intensity measurements $|s(t)|^2$ and $|d(t)|^2$. For ease of discussion, we set $a(t) = |s(t)|$ and $b(t) = |d(t)|$. The solution for the reconstruction of the optical field can be represented as a problem of identifying a phase signal $\angle\tilde{s}(t)$ to satisfy the following equation:

$$\underset{\angle\tilde{s}(k)}{\operatorname{argmin}} \sum_{m=1}^{N} \times \left(\left| \sum_k (a(k) \exp(j\angle\tilde{s}(k)) \cdot h_D(mT - kT) \right| - b(mT) \right)^2. \tag{4}$$

The process of identifying the values of $\angle\tilde{s}(k)$ that minimize the expression in Eq. (4) is realized by the iterative optimization with several physical constraints. Here we propose a solution to the above-mentioned iterative optimization problem, as shown in Algorithm 1, where h_{CD} represents the CD transfer functions of the SSMF transmission. M is the total number of iterations for the PR receiver. h_{RRC} is the root raised cosine (RRC) shaping filter. t'_p is the time slot assigned for pilot symbols x_p. $\otimes$ represents the convolution operation. A random phase ranging from $-\pi$ to π is initialized, and the signal phase is updated after every iteration. Within the iteration loop, the measured signal intensity is first powered by a factor of P, as shown in Fig. 1, and P is adaptively adjusted with respect to the current iteration by a maximal powering factor R and a decaying factor V. The Pth powering operation can be implemented by a look-up-table (LUT) for the efficient hardware implementation. Practically, both R and V need to be optimized for the performance improvement of the PR receiver, in terms of both the convergence speed and the PR accuracy. After the intensity transformation, the transformed signal is still strongly correlated with the original intensity signal. We can treat the intensity transformation as artificially heating data, which is equivalent to the entropy enhancement during the simulated annealing process [12]. With the aid of the intensity transformation, the PR algorithm trapping at the sub-optimal solution can be avoided; thus, better convergence performance can be anticipated. Then the reconstructed signal is propagated back to the Tx by imposing the CD compensation h_{CD}^{-1}. After passing through an RRC filter and being down-sampled to one sample per symbol (Sps), the pilot constraint is implemented to update the phase of the samples at the pre-determined locations [7]. Since the quadrature phase-shift keying (QPSK) format has a constant modulus, another modulus constraint to enforce the signal intensity as a constant is applied. It is worth mentioning that the modulus constraint is also suitable for high-order advanced modulation formats with multiple moduli, such as 16-QAM and 64-QAM signals. Thus, our proposed PR_AIT for the QPSK signal can be applied to other advanced modulation formats after proper modifications. Thereafter, the electrical signal is up-sampled to 2 Sps and RRC shaped. After further propagating to the projection plane, the signal intensity is replaced by the transformed intensity; then the updated signal is propagated to the Rx, and the signal phase is correspondingly updated for the next iteration. Please note that the algorithm is implemented in a block-wise manner with a block size of B, and the signal propagation and the shaping are processed in the frequency domain by using the classical radix-2 algorithm for fast Fourier transform. Assuming the resolution of analog-to-digital converters (ADCs) is n bits, the implementation of PR_AIT algorithm requires MB$(12\log 2(B) + 19)$ real multiplications, 6 MB$(\log 2(B) + 1)$ real adders, and a LUT with a size of $M \times 2^n$.

To verify the performance improvement associated with the proposed PR_AIT receiver, we carry out numerical simulations for single-carrier single-polarization 56 Gbaud (QPSK) signal transmission over the 80 km SSMF, considering the practical implementation noise. Figure 2 shows the simulation setup and the corresponding digital signal processing (DSP) flow. At the Tx, a sequence of 65536 QPSK symbols is first generated with a symbol rate of 56 GBaud. After performing up-sampling, the QPSK signal is RRC shaped with a roll-off factor of 0.01. The electrical-to-optical conversion is realized by an in-phase/quadrature modulator (IQM), and a 1550 nm semiconductor laser with a linewidth of 1 MHz is chosen as the continuous-wave optical carrier. In order to emulate the overall Tx noise characteristic to reach a 23 dB signal-to-noise ratio (SNR), additive white Gaussian noise (AWGN) is loaded to the optical QPSK signal. The transmission link consists of a span of 80 km SSMF with a dispersion parameter of 17 ps/nm/km. After the SSMF transmission, the noise loading module is used to adjust the OSNR of received QPSK signals. Thereafter, the signal is fed into the proposed PR receiver, including an optical splitter, a dispersive element using a dispersion compensating fiber or chirp fiber Bragg grating, and two single-ended PDs whose response is emulated as a 4th-order Bessel filter with a 3 dB bandwidth of 60 GHz, and two ADCs with a resolution of 6 bits and a sampling rate of 112 GSample/s. Once the signal

Algorithm 1. PR_AIT algorithm

Function PR_AIT $(a(t), b(t), R, V, h_{\mathrm{CD}}, h_D, M)$

1. $\angle\hat{s}(t) = \angle\mathrm{rand}(t)$ ◇ Initialize phase
2. **For** i **from 1 to** M
3. $a(t) \leftarrow a(t)^P$, $b(t) \leftarrow b(t)^P$; where $P = (R-1)\cdot\exp(-i/V)+1$ ◇ AIT
4. $\hat{s}(t) = a(t)\exp(j\angle\hat{s}(t))$ ◇ Reconstruct the field
5. $\hat{s}(t) \leftarrow h_{\mathrm{CD}}^{-1}(t) \otimes \hat{s}(t)$ ◇ Propagate back to Tx
6. $\hat{s}(t) \leftarrow h_{\mathrm{RRC}}(t) \otimes \hat{s}(t)$ ◇ RRC matched shaping
7. $\hat{s}(t') \leftarrow \hat{s}(t)$ ◇ Down-sample to 1 Sps
8. $\hat{s}(t'_p) \leftarrow |s_p(t'_p)|\exp(j\angle s_p(t'_p))$ ◇ Pilot constraint
9. $\hat{s}(t') \leftarrow |s_p(t'_p)|\exp(j\angle\hat{s}(t'))$ ◇ Modulus constraint
10. $\hat{s}(t) \leftarrow \hat{s}(t')$ ◇ Up-sample to 2 Sps
11. $\hat{s}(t) \leftarrow h_{\mathrm{RRC}}(t) \otimes \hat{s}(t)$ ◇ RRC shaping
12. $\hat{s}(t) \leftarrow h_{\mathrm{CD}}(t) \otimes h_D(t) \otimes \hat{s}(t)$ ◇ To projection plane
13. $\hat{s}(t) \leftarrow b(t)exp(j\angle\hat{s}(t))$ ◇ Intensity update
14. $\hat{s}(t) \leftarrow h_D^{-1}(t) \otimes \hat{s}(t)$ ◇ Propagate back to Rx
15. Returns $exp(j\angle\hat{s}(t))$

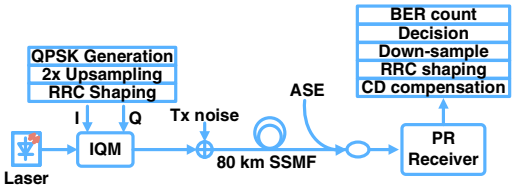

Fig. 2. Simulation setup and corresponding DSP flow.

field reconstruction is realized, the Rx DSP flow, including the CD compensation, the matched RRC filtering, the down-sampling to 1 Sps, the symbol decision, and the BER counting, can be implemented.

First, we investigate the effect of the dispersive element on the performance of the proposed PR receiver under the condition of a 20 dB OSNR, and the achieved BER with respect to the CD value is summarized in Fig. 3(a). For ease of performance comparison, the PR_PR receiver with the phase reset parameter of 10, which is defined as the number of iterations between wo phase resets, is numerically implemented as well [10]. As for both the PR_AIT ($R = 6$, $V = 20$) and PR_PR receivers, the number of total iterations is set at 2000 to ensure the algorithm convergence, and 20% periodically inserted pilot symbols are used. We can find that the performance of both PR receivers improves with the growing CD value of the dispersive element, due to the involvement of more signal symbols. We believe that the introduction of a large CD is helpful to de-correlate two intensity measurements and prevent the PR algorithm from being trapped into the sub-optimal solutions. Moreover, the BER starts to saturate after the use of a sufficiently large amount of CD, such as 8500 ps/nm. Meanwhile, the proposed PR_AIT receiver can ensure a better BER performance under various CD values in comparison with the PR_PR receiver. For ease of discussion, we fix the CD value of the dispersive element at 8500 ps/nm for the next investigations. The relationship between the SSMF reach and the achieved BER is presented in Fig. 3(b). When the SSMF reach varies from 20 to 160 km, we can observe that the BER performance is almost unchanged for both PR receivers, indicating that the selected CD value of the dispersive element is independent of the SSMF reach. Figure 3(c) shows the BER results with respect to the OSNR

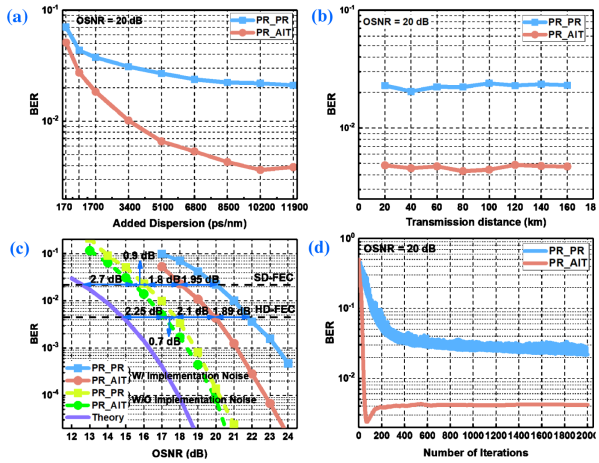

Fig. 3. (a) Achieved BER versus the used CD value arising from the dispersive element in the PR receiver. (b) Achieved BER versus the SSMF reach. (c) Achieved BER versus the OSNR. (d) Achieved BER versus the number of iterations.

after 2000 iterations. The BER performance in theory and that for the two schemes without considering any implementation noise [7] are also presented for ease of comparison. The proposed PR_AIT receiver can significantly reduce the BER, when it is compared with the PR_PR receiver for various OSNRs. In addition, the proposed PR_AIT receiver is more robust to the implementation noise in comparison with the PR_PR receiver. As a result, to reach both the 20% and 7% FEC threshold of $\mathrm{BER} = 2.2 \times 10^{-2}$ and 4.5×10^{-3} [13], respectively, the required OSNRs for the proposed PR_AIT receiver can be reduced by 1.95 and 1.89 dB. However, both the PR_AIT and PR_PR receivers experience a severe performance penalty in comparison with the theoretical curve, because of the occurrence of the practical implementation noise. To investigate the performance of convergence speed, the relationship between the achieved BER and the number of iterations are presented in Fig. 3(d). The proposed PR_AIT receiver has a faster convergence than that of the PR_PR receiver. About 800 iterations are required for the PR_PR receiver to obtain a steady BER performance of around 2.5×10^{-2}, while only around 50 iterations are needed for our proposed PR_AIT receiver to reach a steady BER of around 4×10^{-3}, indicating a 16-time reduction of iteration number. Moreover, an interesting phenomenon of the PR_AIT receiver is that there occurs an optimal number of iterations, which is reflected by a BER dip in Fig. 3(d). We infer that the optimal number of iterations is determined by the AIT parameters and OSNR, due to the interaction between the noise and the intensity signal.

Next, we investigate the PR accuracy by characterizing the mean $|\Delta\theta|$ value as a function of the number of iterations, as shown in Fig. 4(a). $|\Delta\theta|$, which is defined as a symbol-wise absolute phase error between $h_{\mathrm{CD}}^{-1}(t) \otimes \hat{s}(t)$ and the modulated signal $s(t)$, and can be treated as a metric to evaluate the PR accuracy [10]. As shown in Fig. 4(a), the proposed PR_AIT receiver guarantees both faster convergence and higher PR accuracy, which are consistent with our observations in Fig. 3(d). The cumulative distribution function (CDF) of $|\Delta\theta|$ with respect to the number of iterations is also presented in Fig. 4(b). We can clearly observe that the phase error is more centralized at the vicinity of 0 radian for the proposed PR_AIT receiver

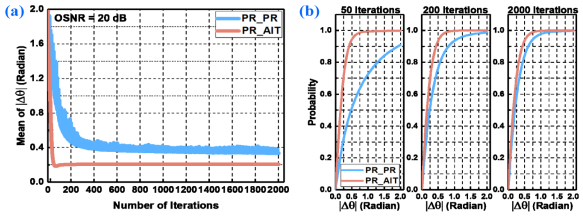

Fig. 4. (a) Mean absolute phase error versus the number of iterations. (b) CDF of the absolute phase error after 50, 200, and 2000 iterations.

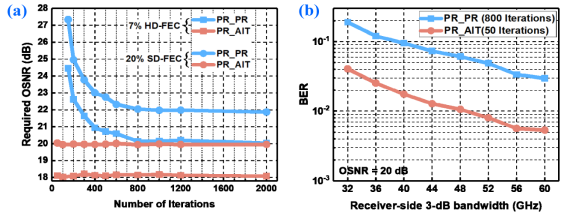

Fig. 5. (a) Required OSNR versus the number of iterations. (b) Impact of an Rx bandwidth on the PR receiver performance.

under various numbers of iterations, indicating excellent PR accuracy. Furthermore, the CDF curve keeps almost unchanged within the iteration range from 50 to 2000, indicating a fast convergence rate for the proposed PR_AIT receiver.

The required OSNR with respect to the number of iterations is summarized in Fig. 5(a). Impressively, the PR_AIT receiver ensures better performance under various numbers of iterations, and the required OSNR keeps stable, which is around 18.1 and 19.95 dB for the 20% and 7% FEC, respectively, when the number of iterations varies from 50 to 2000. In contrast, there is a strong dependence between the required OSNR and the number of iterations for the PR_PR receiver. In particular, more iterations are helpful to obtain a smaller required OSNR for the PR_PR receiver. Additionally, when the number of iterations is below 150, an error-free transmission is prohibited, regardless of the OSNR value. The impact of Rx implementation imperfection is also investigated under the condition of a 20 dB OSNR. The relationship between the achieved BER and the Rx 3 dB bandwidth is shown in Fig. 5(b), where 50 and 800 iterations are set for the PR_AIT and the PR_PR receivers, respectively. The BER performance is degraded with the reduction of the Rx bandwidth for both PR receivers. However, our proposed PR_AIT receiver outperforms the PR_PR receiver under various Rx bandwidths. In addition, almost the same BER can be obtained for the PR_AIT receiver with a 3 dB bandwidth of 34 GHz and the PR_PR receiver with a 3 dB bandwidth of 60 GHz.

Finally, the impact of AIT parameters on the proposed PR_AIT receiver is investigated for various numbers of iterations under the condition of a 20 dB OSNR, as shown in Fig. 6. When the number of iterations is smaller, such as 30, the AIT parameter R and the achieved BER are strongly correlated. With the growing number of iterations, the BER performance dependent on the AIT parameter R gradually becomes weak. In contrast, the achieved BER is strongly dependent on the

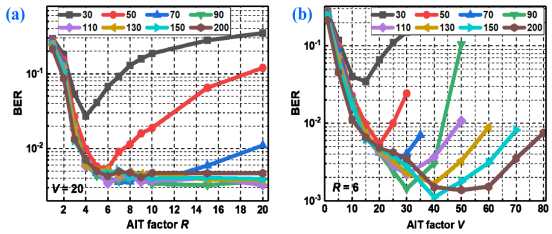

Fig. 6. Impact of the AIT parameter (a) maximal powering factor R and (b) decaying factor V on the PR_AIT receiver performance.

AIT delay parameter V. There always exists an optimal value to ensure a minimal BER for various numbers of iterations. Furthermore, the optimal V is proportional to the number of iterations.

In summary, we have proposed a new carrier-less PR receiver based on the AIT, with the capability of both fast convergence and high PR accuracy. With only 50 iterations, we can numerically reconstruct 56 GBaud QPSK signals after the 80 km SSMF transmission, leading to a 16-time reduction of calculation complexity in comparison with the recently reported the PR_PR receiver. Meanwhile, the proposed PR_AIT receiver can reduce the required OSNR by 1.95 and 1.89 dB, in terms of 20% soft-decision FEC and 7% hard-decision FEC, respectively.

Funding. National Key Research and Development Program of China (2019YFB1803803); National Natural Science Foundation of China (62075046); Hetao Shenzhen-Hong Kong Science and Technology Innovation Cooperation Zone applied fundamental research project (HZQB-KCZYB-2020082).

Disclosures. The authors declare no conflicts of interest.

Data Availability. Data underlying the results presented in this paper are not publicly available at this time but may be obtained from the authors upon reasonable request.

REFERENCES

1. H. Xin, K. Zhang, L. Li, H. Le, and W. Hu, IEEE Photonics Technol. Lett. **32**, 643 (2020).
2. D. Che, Q. Hu, and W. Shieh, J. Lightwave Technol. **34**, 516 (2016).
3. A. Mecozzi, C. Antonelli, and M. Shtaif, Optica **3**, 1220 (2016).
4. C. Sun, D. Che, H. Ji, and W. Shieh, in *Optical Fiber Communication Conference* (2019), paper M1H.6.
5. S. An, Q. Zhu, J. Li, and Y. Su, J. Lightwave Technol. **38**, 485 (2020).
6. G. Goeger, C. Prodaniuc, Y. Ye, and Q. Zhang, in *European Conference on Optical Communications* (2015), paper 0607.
7. H. Chen, N. Fontaine, J. Gene, R. Ryf, D. Neilson, and G. Raybon, J. Lightwave Technol. **38**, 2587 (2020).
8. H. Huang, H. Chen, Y. Huang, N. Fontaine, R. Ryf, and Y. Song, Opt. Lett. **45**, 6070 (2020).
9. Y. Yoshida, T. Umezawa, A. Kanno, and N. Yamamoto, J. Lightwave Technol. **38**, 90 (2020).
10. H. Chen, H. Huang, N. Fontaine, and R. Ryf, Opt. Lett. **45**, 1188 (2020).
11. G. Huang, D. Wu, J. Luo, L. Lu, F. Li, Y. Shen, and Z. Li, Photonics Res. **9**, 34 (2021).
12. S. Kirkpatrick, C. D. Gelatt, Jr., and M. P. Vecchi, Science **220**, 671 (1983).
13. B. Smith, A. Farhood, A. Hunt, F. Kschischang, and J. Lodge, J. Lightwave Technol. **30**, 110 (2012).